Acute perturbation strategies in interrogating RNA polymerase II elongation factor function in gene expression

Bin Zheng, Yuki Aoi, Avani P. Shah, Marta Iwanaszko, Siddhartha Das, Emily J. Rendleman, Didi Zha, Nabiha Khan, Edwin R. Smith, and Ali Shilatifard

Simpson Querrey Institute for Epigenetics, Department of Biochemistry and Molecular Genetics, Feinberg School of Medicine, Northwestern University, Chicago, Illinois 60611, USA

The regulation of gene expression catalyzed by RNA polymerase II (Pol II) requires a host of accessory factors to ensure cell growth, differentiation, and survival under environmental stress. Here, using the auxin-inducible degradation (AID) system to study transcriptional activities of the bromodomain and extraterminal domain (BET) and super elongation complex (SEC) families, we found that the CDK9-containing BRD4 complex is required for the release of Pol II from promoter-proximal pausing for most genes, while the CDK9-containing SEC is required for activated transcription in the heat shock response. By using both the proteolysis targeting chimera (PROTAC) dBET6 and the AID system, we found that dBET6 treatment results in two major effects: increased pausing due to BRD4 loss, and reduced enhancer activity attributable to BRD2 loss. In the heat shock response, while auxin-mediated depletion of the AFF4 subunit of the SEC has a more severe defect than AFF1 depletion, simultaneous depletion of AFF1 and AFF4 leads to a stronger attenuation of the heat shock response, similar to treatment with the SEC inhibitor KL-1, suggesting a possible redundancy among SEC family members. This study highlights the usefulness of orthogonal acute depletion/inhibition strategies to identify distinct and redundant biological functions among Pol II elongation factor paralogs.

[*Keywords*: super elongation complex; BRD4; BRD2; transcription elongation; enhancer activity; heat shock PROTAC; auxin-inducible degradation]

Supplemental material is available for this article.

Received October 27, 2020; revised version accepted December 3, 2020.

Induction of heat shock gene expression was one of the first examples of genes exhibiting promoter-proximal pausing, which was later shown to be a property shared among most Pol II transcribed genes in metazoans (Smith et al. 2011; Adelman and Lis 2012; Chen et al. 2018). For a cohort of heat shock-induced genes, upon heat shock, Pol II is rapidly released into the gene body for productive elongation (Mahat et al. 2016). The release of Pol II from promoter-proximal pausing requires the kinase activity of CDK9, which with its cyclin partner Cyclin T, forms a complex known as positive transcription elongation factor b (P-TEFb) (Lis et al. 2000; Price 2000; Ni et al. 2008). In cells, P-TEFb further interacts with other proteins to form multiple distinct complexes (Peterlin and Price 2006; Zhou and Yik 2006; Smith et al. 2011; Chen et al. 2018). Among them, the 7SK-Hexim complex is a ribonucleoprotein complex that is generally considered to be a reservoir for P-TEFb, while BRD4-P-TEFb and the super elongation complex (SEC) that contains P-TEFb are catalytically active (Nguyen et al. 2001; Yik et al. 2003; Jang et al. 2005; Lin et al. 2010; Luo et al. 2012b).

Bromodomain-containing protein BRD4 is part of the bromodomain and extraterminal domain family along with BRD2 and BRD3, which are ubiquitously expressed, and BRDT, which is testis-specific and most similar to BRD4 (Hsu and Blobel 2017). The BET proteins bind to acetylated lysines of histones through the bromodomain. BET inhibitors that competitively bind the bromodomains of the BET family proteins have been developed (Filippakopoulos et al. 2010; Dawson et al. 2011). These inhibitors prevent BET proteins from binding to acetylated histones and therefore prevent BET proteins from

Corresponding author: ash@northwestern.edu
Article published online ahead of print. Article and publication date are online at http://www.genesdev.org/cgi/doi/10.1101/gad.346106.120.

efficient recruitment to chromatin. Myc is widely considered to be a downstream target of BRD4, through binding of BRD4 to the promoter and enhancers of the *MYC* gene (Zuber et al. 2011; Lovén et al. 2013). PROTAC versions of BET inhibitors have also been developed, which fuse a chemical ligand for an E3 ligase to a BET inhibitor that resulted in a rapid degradation of the BET proteins (Lu et al. 2015b; Winter et al. 2015). BRD4 and its testis-specific paralog BRDT are the only BET proteins that bind to P-TEFb due to a C-terminal sequence not present in the other BET proteins (Bisgrove et al. 2007). Depletion of the BET family proteins with the proteolysis targeting chimera (PROTAC) dBET6 results in global promoter-proximal pausing of Pol II, which was assumed to be due to the loss of BRD4, since it interacts with P-TEFb (Winter et al. 2017). However, BET proteins also maintain an active chromatin state at enhancers, and enhancers are important regulators of the release of Pol II from pausing (Hsu and Blobel 2017; Chen et al. 2018). Enhancers are distal regulatory elements that are located upstream of or downstream from their target genes (Schoenfelder and Fraser 2019). Features of enhancers include the binding of transcription factors, histone modifications such as monomethylation of H3 lysine 4 (H3K4me1), and acetylation of H3 lysine 27 (H3K27ac) (Li et al. 2016). It has been proposed that enhancers carry out *cis*- and *trans*-regulations either through chromatin looping and/or enhancer transcription (eRNA) (Andersson and Sandelin 2020). The importance of BET protein binding at enhancers was first suggested from the use of BET inhibitors, which led to reduced enhancer activity that was attributed to BRD4 function (Kanno et al. 2014). However, BRD2 has been reported to have roles at gene distal regulatory elements, with BRD2 contributing to the formation of transcriptional boundaries with CTCF in murine erythroblast cells (Hsu et al. 2017).

The super elongation complex is built upon the scaffolding proteins AFF1 or AFF4, which interact with the Cyclin T subunit of P-TEFb, along with ELL2 or ELL3, EAF1 or EAF2, and AF9 or ENL (He et al. 2010; Lin et al. 2010; Schulze-Gahmen et al. 2013; Chen et al. 2018). Many of the SEC subunits are translocation partners of MLL in MLL-rearranged leukemias, and these chimeric proteins are thought to function through aberrant recruitment of the SEC to MLL target genes (Lin et al. 2010; Smith et al. 2011). The SEC is also co-opted by the HIV transactivator Tat to promote viral replication (He et al. 2010; Sobhian et al. 2010). Endogenous genes regulated by the SEC include the induction of HOX gene transcription in response to retinoic acid and *HSP70* expression upon heat shock (Lin et al. 2011). Disruption of the AFF4-Cyclin T interaction using a small molecule inhibitor resulted in a reduced rate of transcription elongation and an impaired heat shock response (Liang et al. 2018).

Here, we sought to compare the functions of the SEC and BET transcription factor families by using the auxin-inducible degron system (AID) to rapidly deplete cells of targeted proteins (Nishimura et al. 2009; Natsume et al. 2016). We found that CDK9-containing BRD4 is required for genome-wide release of Pol II from promoter-proximal pausing under normal conditions but is dispensable for Pol II release from pausing during the heat shock response. While we saw a handful of genes that show increased Pol II occupancy at the gene body upon depletion of BRD2, overall, the loss of BRD2 and BRD3 has relatively mild effects on either steady state transcription or the heat shock response. In contrast, depletion of BRD2 leads to global loss of Pol II at enhancers, which is also reflected by dBET6 treatment. While depletion of CDK9-containing SEC has little effect on genome-wide release of Pol II from promoter-proximal pausing, we found that the release of Pol II from pausing is dramatically impaired during the heat shock response. Although depletion of the AFF4 subunit of the SEC affects the heat shock response more than AFF1 depletion, depletion of both proteins more severely attenuates the heat shock response, demonstrating some level of redundancy in these SEC scaffolding proteins.

Results

Depletion of the CDK9-containing BRD4 complex leads to genome-wide promoter-proximal pausing of RNA polymerase II

To investigate the direct effects of BRD4 and its homologs (BRD2 and BRD3) on steady-state transcription by RNA polymerase II, we knocked in a C-terminal mini-AID tag (mAID) for each of these genes using CRISPR. Neomycin and hygromycin selection were used to facilitate the identification of homozygous knock-in clones (Fig. 1A). Auxin treatment in these cell lines triggers rapid degradation of each BET protein with substantial depletion by 2 h, without disturbing the stability of the other family members (Fig. 1B; Supplemental Fig. S1A). As expected, treatment with the PROTAC dBET6 in parental DLD-1 cells leads to degradation of all BET proteins (Fig. 1B). Since BRD2 levels were higher after 24-h auxin treatment than the 2-h auxin treatment of BRD2-AID cells, and dBET6 treatment of wild-type cells for 24 h also had higher BRD2 levels than 2-h dBET6 treatment, we chose the 2-h time point of auxin and dBET6 treatments for further experiments.

We raised an antibody against the mAID tag, which allowed us to compare the relative protein levels of the three BET proteins in cell extracts and their relative occupancy on chromatin (Supplemental Fig. S1B,C). BRD2 is at least five times more abundant than BRD3 and BRD4 as assessed by both Western and ChIP-seq analysis (Fig. 1C, D; Supplemental Fig. S1B,C). Occupancy levels of each BET protein largely follow H3K27ac levels (Fig. 1C). Accordingly, all three BET proteins have similar binding patterns in the genome (Fig. 1D). However, BRD4 has the highest percentage of peaks at promoter regions, while BRD2 has the highest percentage of peaks at intronic and inter-genic regions. BRD2, as the most abundant BET protein, binds to almost every region where BRD3 and BRD4 are found. BRD3 and BRD4 have >40%–60% peak overlap with each other (Fig. 1D). The lower percent overlap between BRD3 and BRD4 peaks compared with either of them with BRD2 peaks could be the result of

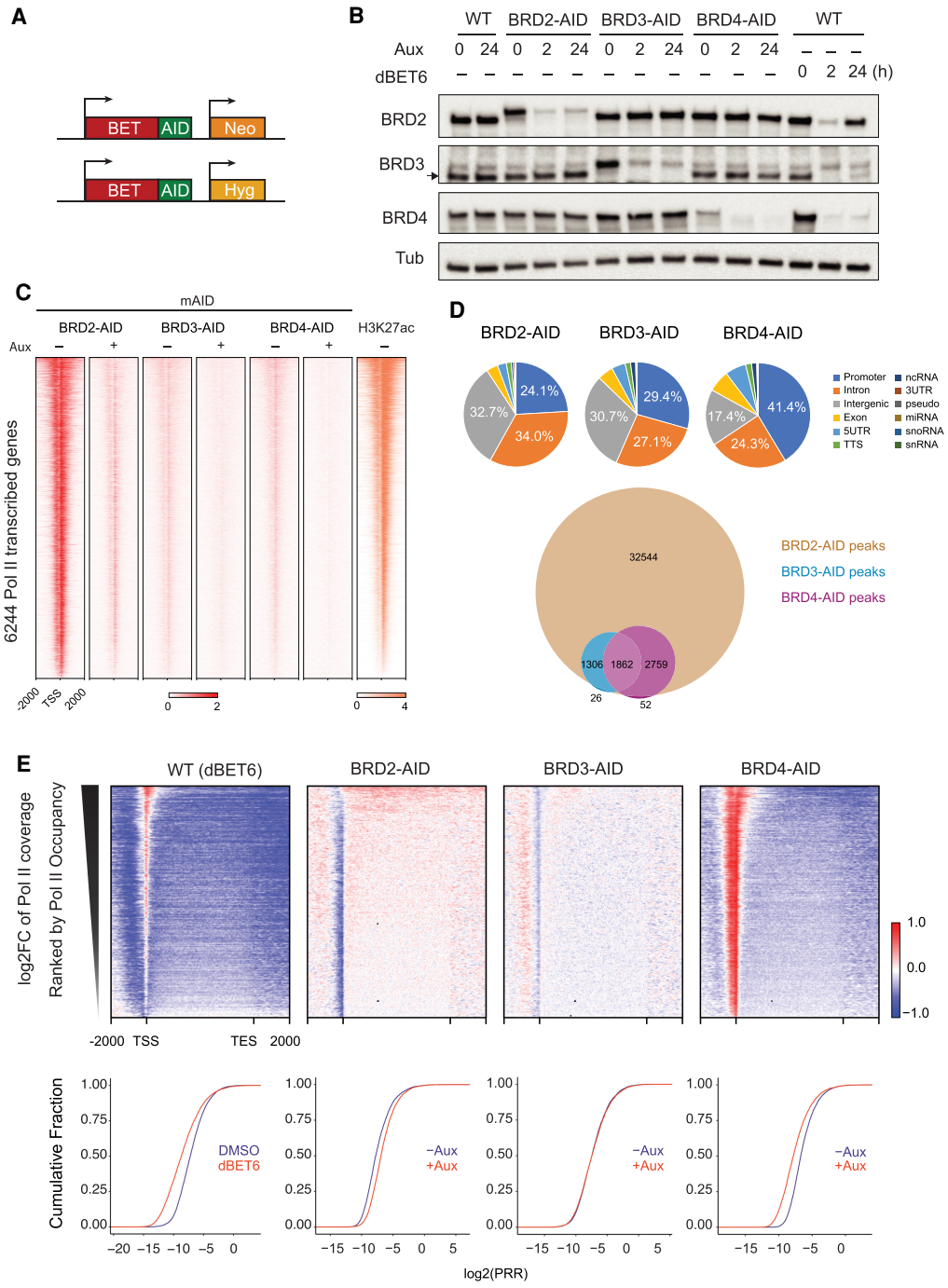

Figure 1. BET bromodomain protein BRD4 is required for global basal transcription by RNA polymerase II. (*A*) Design of BET protein degrons. CRISPR-mediated introduction of the mAID tag into BET proteins BRD2, BRD3, and BRD4. Cotransfection of donor plasmids bearing neomycin and hygromycin are used to ensure the selection of homozygous knock-in clones. (*B*) Western blot analysis showing the degradation of each BET protein in each of the degron cell lines at 2-h and 24-h auxin treatment showing the specific knockdown of the tagged protein, while treatment with dBET6 (250 nM) for 2 h and 24 h leads to degradation of BRD2, BRD3, and BRD4. (*C*) Heat map of mAID and H3K27ac occupancy around the TSS of 6244 Pol II transcribed genes ranked by the H3K27ac signal. Note that BRD3 and BRD4 have much lower occupancy on chromatin than BRD2, consistent with what is seen with the mAID antibody in Western analysis (see Supplemental Fig. S1B). (*D*) Peak annotations of mAID ChIP-seq for the BET proteins at different locations in the genome. Venn diagram showing the overlap of the three BET proteins, with most of the peaks for the less abundant BRD3 and BRD4 overlapping with the peaks called for the much more abundant BRD2. (*E*) ChIP-seq analysis of Pol II occupancy ±auxin or dBET6-mediated BET protein degradation (heat maps ranked by Pol II occupancy in parental cells). ECDF plots (*bottom* panels) show that BRD4 degradation, either through dBET6 treatment or auxin-inducible degradation, leads to a widespread increase in promoter-proximal pausing of Pol II, while BRD2 depletion leads to the release of Pol II into gene bodies for a subset of genes.

BRD3 and BRD4 being much less abundant, and therefore, there is a lower probability of meeting the significance threshold for peak calling. However, we cannot rule out some biological explanation for preferential occupancy of BRD3 or BRD4 at particular locations of the genome.

We performed Pol II ChIP-seq for the three BET degron cell lines after 2 h auxin treatment along with dBET6 treatment in parental DLD-1 cells. BRD4 depletion leads to thousands of genes exhibiting increased paused Pol II at promoter-proximal regions and less Pol II in gene bodies, which can be seen by the leftward shift of the empirical cumulative distribution function (ECDF) plots of the pause release ratio in auxin-treated BRD4 mAID cells and with dBET6 treatment (Fig. 1E; Supplemental Fig. S1D). CDK9 protein levels on chromatin remain unchanged after depletion of BET proteins (Supplemental Fig. S1A), in line with the recent studies showing that BRD4 depletion causes genome-wide down-regulation of gene expression and that the recruitment of CDK9 is independent of BRD4 (Winter et al. 2017; Muhar et al. 2018). While BRD3 depletion has minimal effect on the profile of Pol II, BRD2 depletion results in increased Pol II occupancy for hundreds of genes (Fig. 1C; Supplemental Fig. S1D).

BRD2 depletion results in loss of Pol II at BET-bound enhancers

BET family proteins are known for their high affinity for acetylated histones found both at promoters and enhancers. We therefore evaluated BET protein occupancy at enhancer regions. To isolate putative enhancer regions bound by BET proteins, we first overlapped the peaks from mAID ChIP-seq in BET degron cells with annotated genes to obtain inter-genic BET-bound peaks. We then merged inter-genic peaks to obtain 8421 inter-genic regions bound by one or more BET proteins (Fig. 2A). To separate potential unannotated promoters from enhancers, we clustered H3K27ac, H3K4me1, and H3K4me3, with clusters 2 and 3, comprising 8149 regions, showing a chromatin signature of enhancers (Fig. 2B). We validated the specificity of mAID ChIP-seq at these enhancers and found broad reduction of mAID signal in all three BET-AID cells upon auxin treatment (Fig. 2C). Looking at Pol II occupancy changes upon auxin treatment, we found that BRD2-AID cells showed a broad reduction of Pol II at enhancers, a property that was also seen with dBET6 treatment in parental cells, while BRD3 and BRD4 depletion showed no significant difference (Fig. 2D–F). This is in contrast to what we observe at promoter regions, where Pol II pausing upon dBET6 treatment is mainly due to BRD4 loss (Fig. 1E; Supplemental Fig. S1D). Thus, dBET6 treatment phenocopies Pol II changes at enhancers, seen by auxin-mediated depletion of BRD2 and Pol II changes at promoters upon auxin-mediated BRD4 depletion.

To confirm a role of BRD2 in enhancer activity in another cell type, we also used an HCT-116 BRD2-AID cell line, which we had previously made but had sidelined for further investigation due to more severe predegradation in the absence of auxin (Supplemental Fig. S2A), an issue that has since been described and for which strategies to prevent this drawback have been published (Li et al. 2019; Sathyan et al. 2019). Nonetheless, despite some predegradation, the same phenomenon was observed in the BRD2-AID HCT-116 cell line with a time-course of auxin treatment (Supplemental Fig. S2B–D). Notably, the 24-h treatment of auxin in BRD2-AID brings back the Pol II occupancy slightly, probably due to the coming back of the BRD2 protein, a feature shared in DLD-1 cells (Supplemental Fig. S1B).

Depletion of the CDK9-containing BRD4 complex does not alter rapid transcriptional induction by heat shock

To determine whether BET protein depletion also affects transcription upon cellular stress, we performed Pol II ChIP-seq for BET degron cells before and after heat shock for 1 h at 42°C. Cells were pretreated with or without auxin for 2 h at 37°C before instant heat shock with 42°C preconditioned media (Fig. 3A; Mahat and Lis 2017). Heat shock for 1 h successfully induced the heat shock response in DLD-l cells (Fig. 3B). Known heat shock-induced genes such as the heat shock protein cochaperone *BAG3*, *HSPA8*, and *SERPINH1* (HSP47) can be seen to be induced to wild-type levels in BRD2-, BRD3-, and BRD4-depleted cells (Fig. 3C), indicating the dispensable role of BRD4 or other BET proteins in the rapid transcriptional induction of these genes in response to heat shock. A robust heat shock response was also observed in RNA-seq after depleting cells of BRD4 by RNAi (Hussong et al. 2017) as well as in our own BRD4-AID cells after 4-h heat shock upon BRD4 depletion (Supplemental Fig. S3D).

To confirm that the heat shock response is not impaired by BET protein depletion, we first identified heat shock-inducible genes by *k*-means clustering of the $\log_2$ fold change of Pol II occupancy in 42°C versus 37°C in wild-type DLD-1 cells, which identified a group of 227 genes induced by heat shock (Supplemental Fig. S3A,B). We used this HS gene list to examine the effects of BET depletion on the heat shock response by metagene analysis and ECDF analysis of the $\log_2$ FC of the pause-release ratio (PRR), which measures the proportion of Pol II in gene bodies relative to promoter-proximal Pol II. A similarly robust heat shock response is seen in BRD2-, BRD3-, or BRD4-depleted or control cells (Fig. 3D; Supplemental Fig. S3C). We also checked the HSP70 protein level in BRD4-AID cells upon heat shock for 6 h. A stable HSP70 protein induction was observed in all three independent replicates regardless of the fact that the induction level varies (Fig. 3E,F).

The SEC is required for rapid transcriptional induction by heat shock

AFF1 and AFF4 are scaffolding proteins for the SEC (Lin et al. 2010; He et al. 2011) that result in one of the most active forms of CDK9 (Luo et al. 2012a). Previous studies had shown that components of the SEC are recruited to genes upon rapid induction by retinoic acid, and serum stimulation, as well as heat shock, and that AFF4

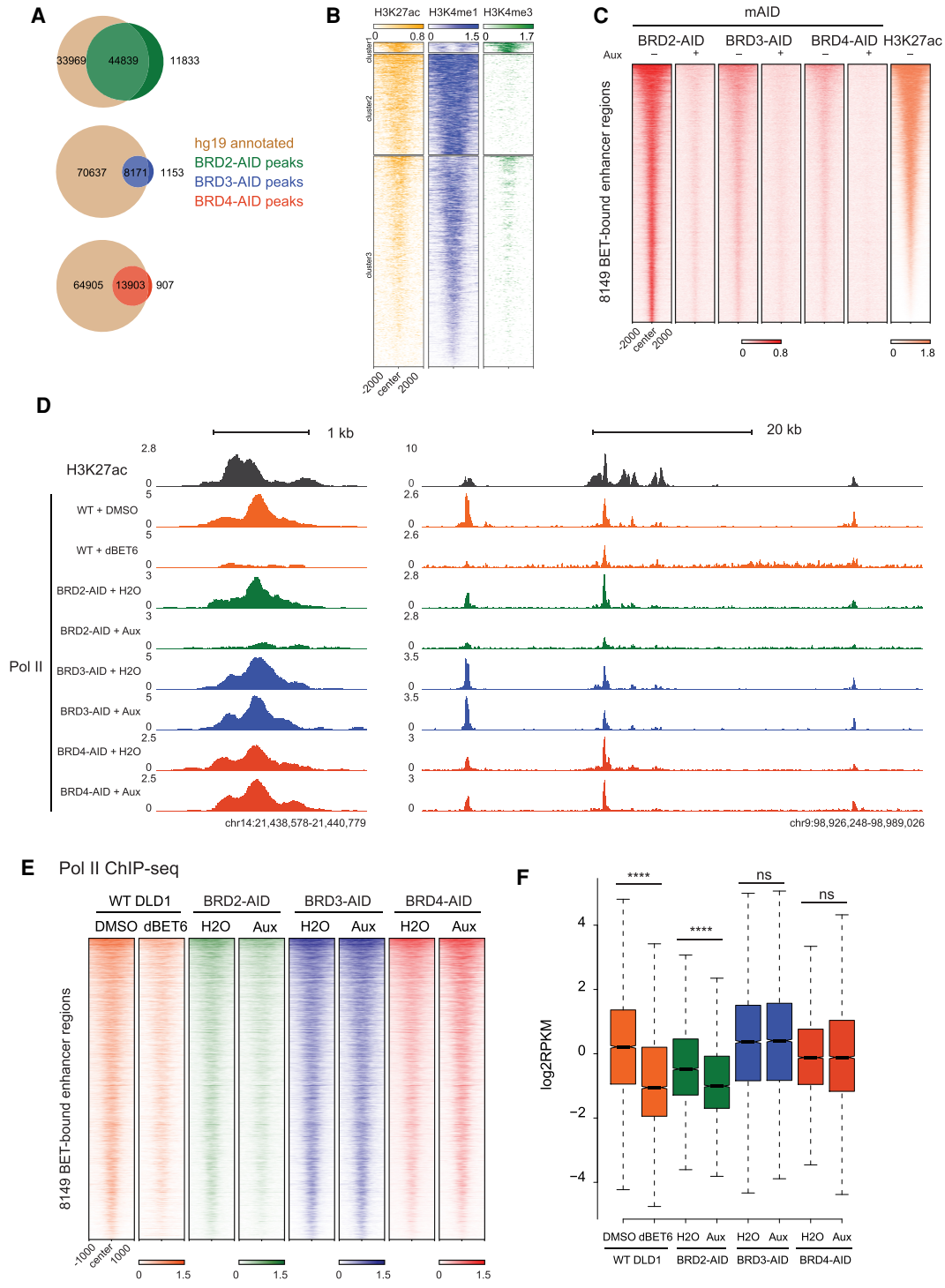

Figure 2. BRD2 depletion results in loss of Pol II at BET-bound enhancers. (*A*) Venn diagram showing the overlap between each BET protein and the UCSC annotated hg19 coding gene regions. Note that BRD4 has the lowest percentage of inter-genic peaks, while BRD2 has the highest percentage of inter-genic peaks (Fig. 1D). (*B*) Clustering of H3K27ac, H3K4me1, and H3K4me3 ChIP-seq at the 8421 inter-genic peaks called for one or more of the BRDs using the mAID antibody. (*C*) Heat map of mAID ChIP-seq ± auxin for BET proteins and sorted by H3K27ac occupancy at the enhancer regions defined by clusters 2 and 3. (*D*) Genome browser views of Pol II ChIP-seq at two different enhancer regions upon auxin treatment in BET degron cells and dBET6 treatment in parental DLD-1 cells for 2 h. H3K27ac ChIP-seq is shown for comparison. (*E*) Heat map of Pol II ChIP-seq at enhancer regions before and after auxin treatment in BET degron cells or dBET6 treatment in parental DLD-1 cells for 2 h. (*F*) Box plot showing the $\log_2$RPKM of Pol II ChIP-seq corresponding to the conditions in *E*. Auxin treatment in BRD2-AID cells and dBET6 treatment in parental cells exhibit significant reductions in Pol II occupancy at enhancer regions. (****) $P < 2.210 \times ^{-16}$, (ns) not significant. Mann–Whitney *U*-test.

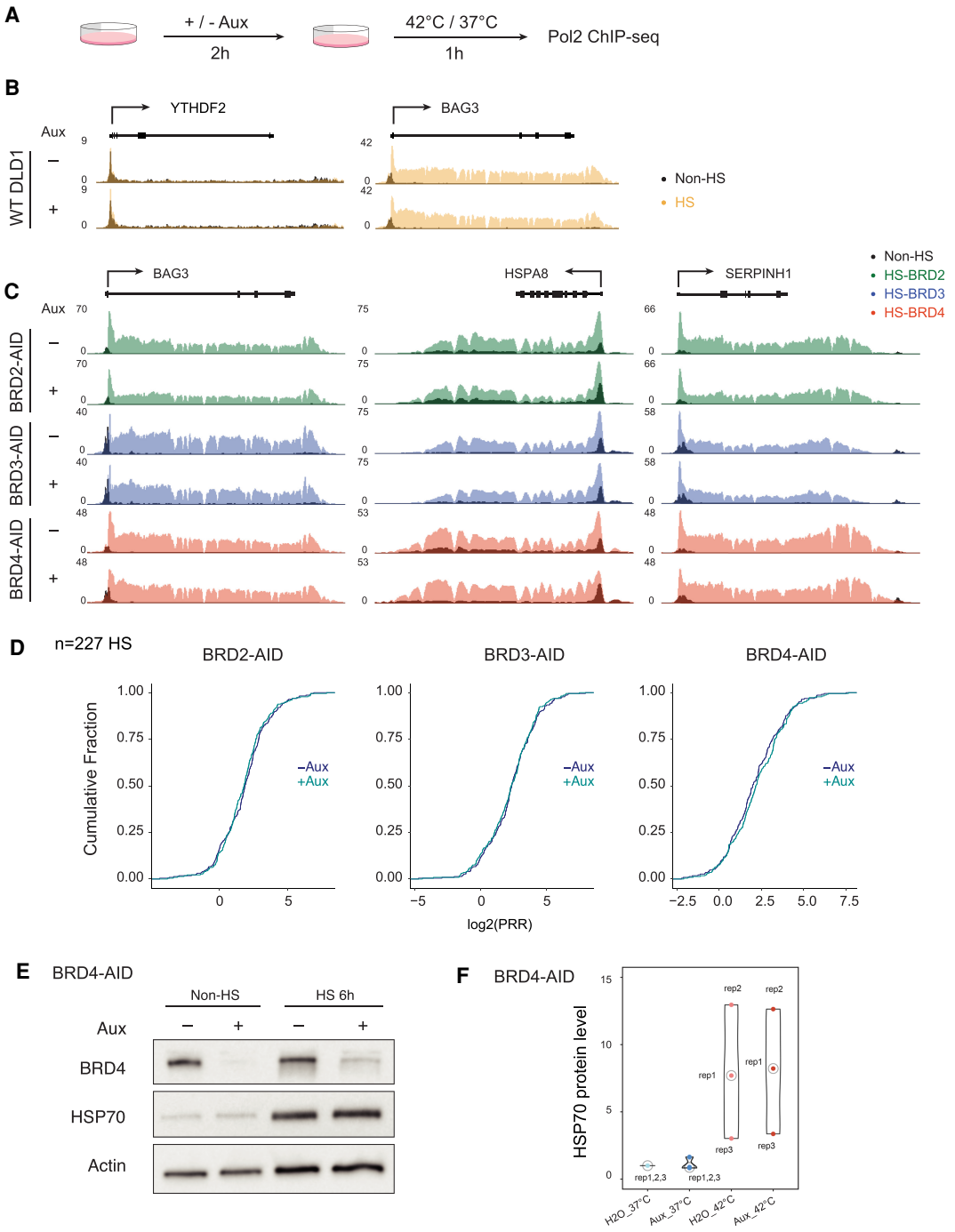

Figure 3. BET proteins are not required for rapid transcriptional induction by the heat shock response. (*A*) Schematic showing that DLD-1 cells were treated with or without auxin for 2 h followed by heat shock for 1 h at 42°C before processing cells for ChIP-seq of Pol II. (*B*) Genome browser overlays of Pol II occupancy at representative non-heat shock (*YTHDF2*) and heat shock-induced (*BAG3*) genes in the 42°C condition in parental DLD-1 cells before (dark color) and after (light color) heat shock. (*C*) Genome browser overlays of Pol II occupancy at the representative heat shock genes in BET degron cells ±auxin for 2 h, followed by non-heat shock (dark color) and heat shock for 1 h (light color). (*D*) ECDF plots of the $\log_2$ pause release ratio (PRR) of the 227 HS-induced genes in BET degron cells ±auxin for 2 h, followed by heat shock for 1 h. A decreased heat shock response due to BET protein depletion would be expected to show a leftward shift of the ECDF curves after auxin treatment. (*E*) Western blots showing normal HSP70 induction after 6-h heat shock in the absence of BRD4. Cells were treated with H_2O or auxin for 2 h at 37°C before 42°C heat shock for 6 h. (*F*) Quantification of HSP70 protein levels ± auxin for three independent replicates as in *E*. Western signal intensity of HSP70 was first converted to fold change of actin within groups and then normalized to the condition of H_2O treatment without heat shock. Circled dots represent the median. While each replicate showed a different level of HSP70 induction, the overall level of induction for each replicate was the same for H_2O and auxin treatments. Replicate 1 is shown in *E*.

knockdown impaired the expression of the heat shock-induced gene *HSP70* by qPCR (Lin et al. 2011; Luo et al. 2012a). Since the CDK9-containing BDR4 complex is not required for rapid transcriptional induction in response to heat shock, we examined the role of CDK9-containing SEC in mediating the heat shock response. We used the same strategy of mAID-mediated depletion of AFF1 and AFF4 (Fig. 4A). Due to the lower abundance of AFF1 and AFF4, we assayed protein levels of AFF1 and AFF4 using nuclear extracts. AFF1 and AFF4 were rapidly and efficiently degraded as seen by Western blotting using commercially available antibodies (Fig. 4B). We also confirmed their efficient degradation using our homemade mAID antibody, which also revealed that AFF4 is expressed at higher levels than AFF1 in DLD-1 cells (Supplemental Fig. S4A).

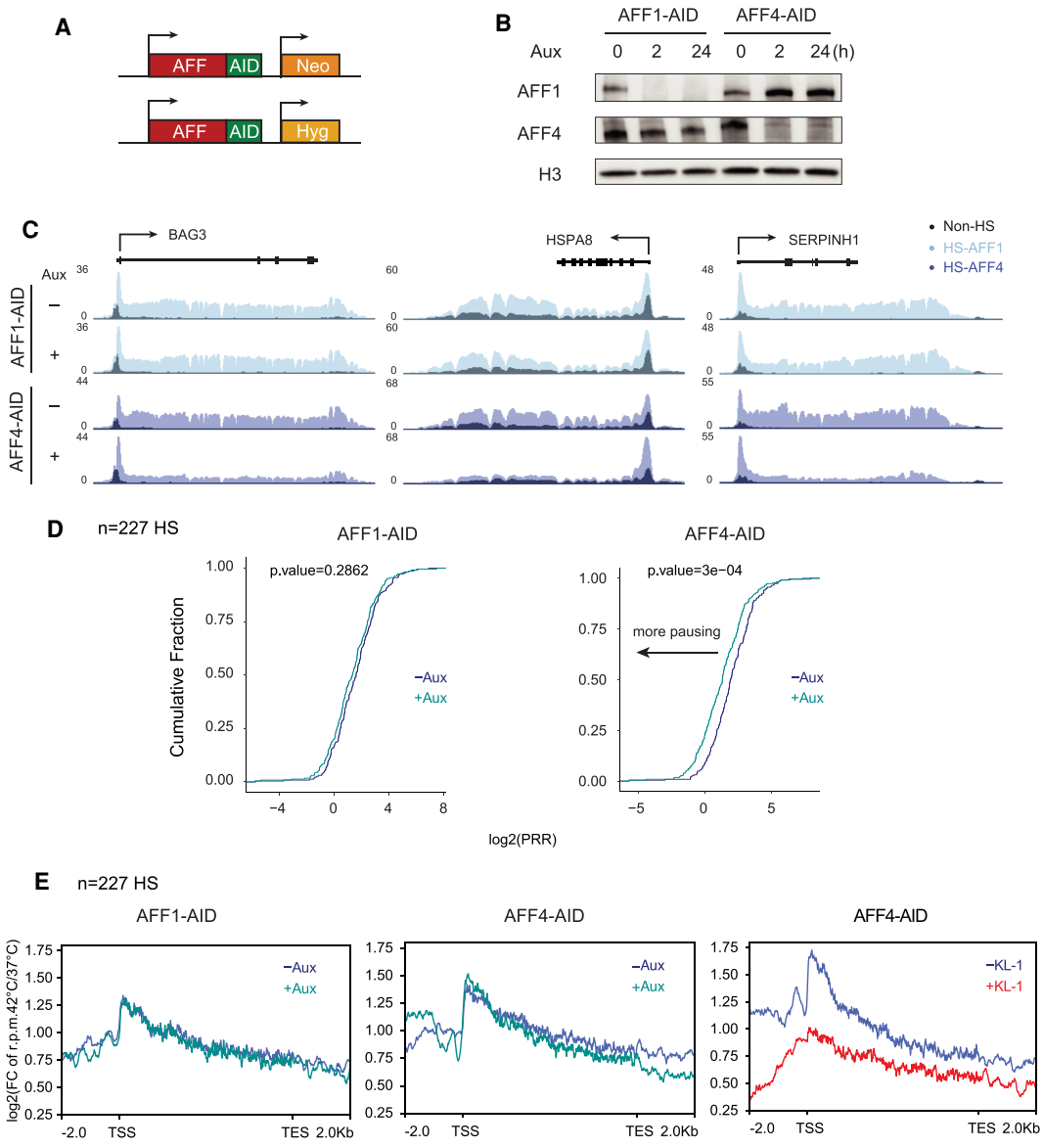

Figure 4. The AFF4 form of the super elongation complex is preferentially required for rapid transcriptional induction upon heat shock. (*A*) Design of auxin degron tagging of the super elongation complex (SEC) scaffolding proteins, AFF1 and AFF4. AFF1-AID and AFF4-AID single degron cells were generated independently using the double selection strategy shown for the BET degron cells. (*B*) Western blotting with the indicated antibodies shows the degradation of nuclear AFF1 or AFF4 in the corresponding degron cells within 2 and 24 h of auxin treatment. (*C*) Genome browser overlay of Pol II occupancy at the representative heat shock-induced genes before (dark color) or after 1h heat shock (light colors) in AFF1 or AFF4 degron cells ±auxin for 2 h. (*D*) ECDF plots of the $\log_2$ fold change of PRR for the 227 HS-induced genes after 1 h heat shock. AFF4 depletion by auxin treatment leads to reduced heat shock induction as indicated by the leftward shift in the PRR, while AFF1 depletion by auxin treatment does not affect heat shock induction. (*E*) Metagene analysis of the $\log_2$ fold change (FC) of Pol II occupancy of 42°C over 37°C for the 227 HS-induced genes ±auxin for 2 h in AFF1-AID and AFF4-AID cells or ±6-h KL-1 (20 µM) treatment in AFF4-AID cells.

We performed Pol II ChIP-seq in the AFF1 and AFF4 degron cells before and after heat shock. AFF1 depletion does not affect the heat shock response, as seen at representative HS genes, while defects at these same genes can be seen after AFF4 depletion, with more promoter-proximal paused Pol II and less Pol II traveling in gene bodies (Fig. 4C). Genome-wide HS analysis by ECDF shows a leftward shift of the curve upon heat shock for AFF4 but not for AFF1, indicating a broad role of SEC/AFF4 in regulating Pol II release in the context of heat shock (Fig. 4D). Both AFF1 and AFF4 are recruited along with Pol II to promoters and gene bodies of HS-induced genes (Supplemental Fig. S4B–D). Despite AFF1 being recruited to HS genes along with AFF4, depleting cells of AFF1 did not impair the release of Pol II into gene bodies upon heat shock (Fig. 4C–E).

The effect of depleting AFF4 in DLD-1 cells was as strong an inhibition of the heat shock response as we previously observed with the SEC inhibitor KL-1 in 293T cells (Liang et al. 2018). We therefore treated DLD-1 cells with the SEC inhibitor for 6 h before performing 1-h heat shock and Pol II ChIP-seq. We found greater inhibition of the heat shock response using KL-1 than depleting AFF4 using the mAID system (Fig. 4E). Therefore, we considered that both AFF1 and AFF4 function in the heat shock response, but since AFF4 is more abundant than AFF1 (Supplemental Fig. S4A), AFF4 can compensate for AFF1 loss better than AFF1 can compensate for AFF4 loss; however, a proper heat shock response cannot occur in the absence of both AFF1 and AFF4.

To address potential redundancy in AFF1 and AFF4 function, we generated a dual homozygous AFF1-AFF4 mAID knock-in cell line (Fig. 5A). As with the single mAID knock-in cells, AFF1 and AFF4 were depleted within 2 h of auxin treatment (Fig. 5B). By metagene analysis of the 227 HS-induced genes (Fig. 5C; Supplemental Fig. S5A) or by examining known heat shock genes (Fig. 5D; Supplemental Fig. S5B), dual depletion of AFF1 and AFF4 with auxin severely attenuates the heat shock response similarly to KL-1 treatment, as can be seen at known heat shock-induced genes (Fig. 5D). Heat map analysis shows similar impairment by either simultaneous AFF1 and AFF4 depletion or with KL-1 treatment for the 227 HS-induced genes. (Fig. 5E). Heat shock-induced genes affected by auxin or KL-1 treatment show considerable overlap (Fig. 5F). Consequently, the mRNA level of representative heat shock genes was severely reduced upon dual depletion of AFF1 and AFF4 after 4-h heat shock (Supplemental Fig. S5C), and HSP70 protein level in AFF1/4-AID cells upon heat shock for 6 h was dramatically reduced regardless of the various induction levels among replicates (Fig. 5G,H).

Discussion

In this study, we used the auxin-inducible degron (AID) system and applied acute perturbation strategies to study the transcription factor family function with a focus on SEC and BET protein complexes. We found that depletion of the CDK9-containing BRD4 complex leads to a genome-wide increase in pausing of Pol II, while BRD2 depletion results in broad loss of Pol II at enhancers, and each of these activities is also seen with the BET PROTAC, dBET6. We also found that the CDK9-containing BRD4 complex, BRD2, and BRD3 are dispensable for the heat shock response in DLD-1 cells. However, the CDK9-containing SEC is essential for a proper heat shock response in these cells.

It is important to point out that, in the absence of the SEC, there is still a significant induction of heat shock genes, just not the full heat shock response seen in wild-type cells that presumably is optimal for cell survival under stress. This residual induction of heat shock gene expression could be due to the remaining SEC observed by Western analysis after auxin treatment, or it is possible that, in the absence of the SEC, BRD4-P-TEFb partially compensates in the release of paused Pol II upon heat shock. We did observe that, in the non-heat shock condition, BRD4 depletion led to more pausing at heat shock-inducible genes just like other non-heat shock genes, indicating that BRD4-P-TEFb is the predominant form of P-TEFb until the recruitment of the SEC upon heat shock. The preferential recruitment of the SEC form of P-TEFb and not BRD4-P-TEFb to heat shock genes could be due to the ability of the SEC to contribute to a more robust heat shock response. The SEC has been shown to be a more active form of P-TEFb in vitro using fractionated nuclear extracts (Luo et al. 2012a). In addition, the SEC contains ELL2, which is an RNA processivity factor that can also facilitate full levels of heat shock gene induction (Shilatifard et al. 1996, 1997; Smith et al. 2008).

In addition to answering the question of why the SEC is recruited to heat shock genes, it will also be important to answer how the SEC is preferentially recruited to heat shock genes upon heat shock. The SEC could conceivably be recruited to heat shock genes through a direct interaction with the master transcription factor for heat shock genes, HSF1, analogously to the direct recruitment of the SEC to the HIV LTR by the HIV transactivator Tat protein (Lu et al. 2015a). However, the SEC has also been shown to interact with the metazoan-specific Mediator protein MED26, which can facilitate SEC recruitment to heat shock genes (Takahashi et al. 2011).

Stabilizing mutations of AFF4 in a SIAH E3 ligase-dependent degron motif are responsible for the developmental syndrome CHOPS (Izumi et al. 2015), and a similar spontaneous stabilizing mutation in mouse AFF1 (AF4) had several developmental defects (Bitoun and Davies 2005), thus highlighting the importance of controlling the protein levels of SEC scaffolding proteins during development. AFF2 and AFF3 are also SEC scaffolding proteins with more restricted expression (Luo et al. 2012a). Indeed, since AFF2 and AFF3 are not expressed in DLD-1 cells, we have not yet looked at their roles in rapid transcriptional induction. It will be interesting to determine which forms of the SEC are needed for the timely response to developmental cues, analogously to the requirement for AFF1 and AFF4 in the response to heat shock as examined in this study.

In addition to finding a role for the BRD4 form of P-TEFb in basal transcription and the SEC in activated

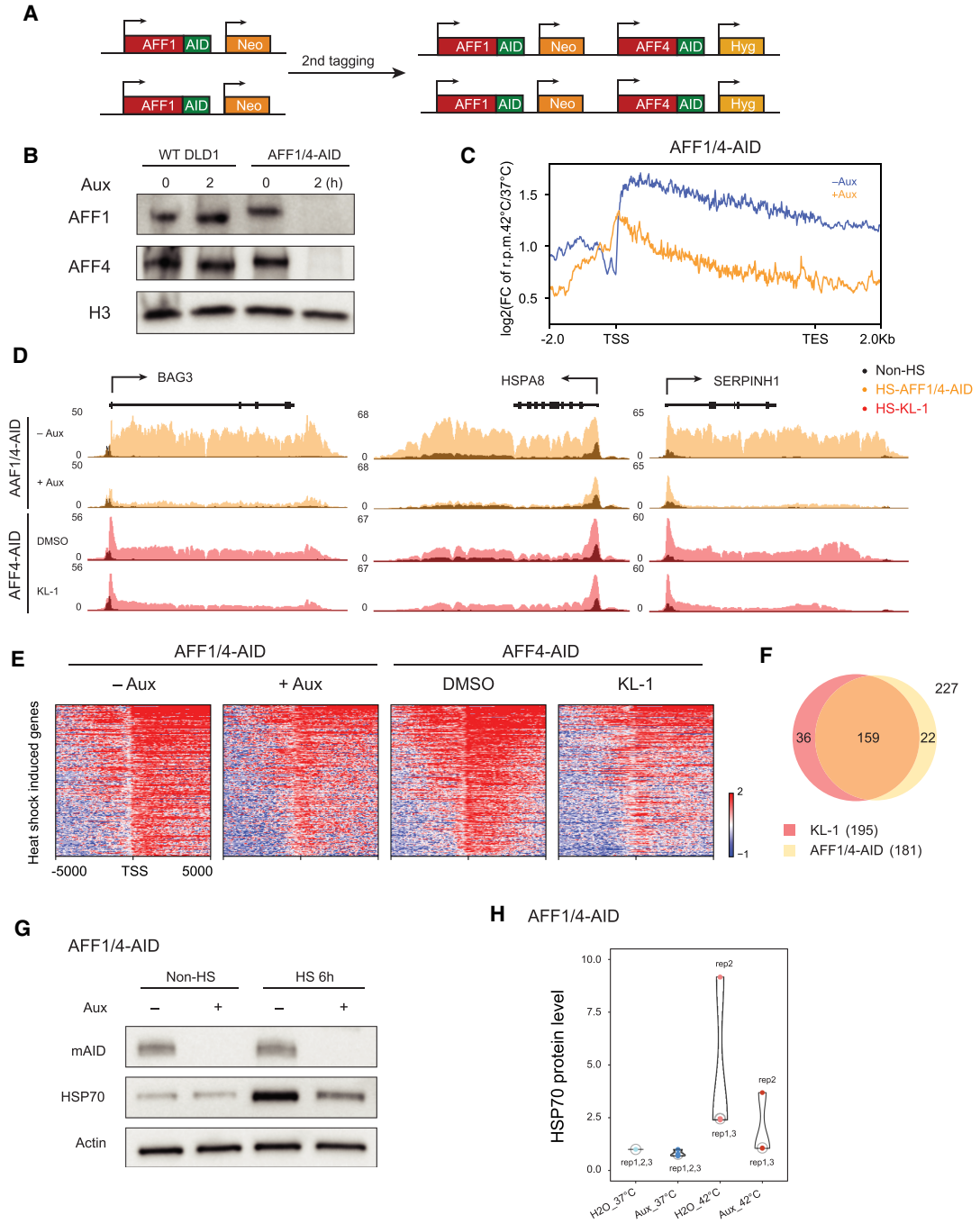

Figure 5. The SEC is essential for rapid transcriptional induction by heat shock. (*A*) Design of AFF1-AFF4 double degron DLD-1 cells. Neomycin was used for selection of AFF1-AID homozygous knock-in clones, which were subsequently used for a homozygous knock-in of the mAID tag for *AFF4* using hygromycin selection. (*B*) Western blot analysis demonstrating the degradation of both AFF1 and AFF4 after auxin treatment for 2 h, compared with the parental DLD-1 cells. (*C*) Metagene analysis showing the $\log_2$FC of Pol II occupancy of 42°C over 37°C for the 227 HS-induced genes before and after simultaneous depletion of AFF1 and AFF4. Decreased induction of Pol II occupancy in the gene bodies during heat shock is observed. (*D*) Genome browser overlay of Pol II occupancy at representative heat shock genes before (dark color) and after (light color) heat shock for 1 h, ±auxin depletion of AFF1 and AFF4 for 2 h, or KL-1 treatment (20 µM) for 6 h. (*E*) Heat map showing the $\log_2$ fold change of Pol II coverage around the TSS for the 227 HS-induced genes for auxin treatment of the AFF1–AFF4 double degron cells and KL-1 treatment of AFF4 degron cells. (*F*) Venn diagram showing the overlap of the 227 HS-induced genes whose induction is impaired by auxin depletion of AFF1 and AFF4 or by KL-1 treatment or both treatments. (*G*) Western blotting with the indicated antibodies showing attenuated HSP70 induction after 6-h heat shock after dual depletion of AFF1 and AFF4. Cells were treated with H2O or auxin for 2 h at 37°C before 42°C heat shock for 6 h. (*H*) Quantification of HSP70 protein levels ±auxin for three independent replicates as in *G*. Western signal intensity of HSP70 was first converted to fold change of actin within groups and then normalized to the condition of H2O treatment without heat shock. Circled dots represent the median. Replicate 2 is shown in *G*.

transcription, we uncovered a role for BRD2, but not BRD3 or BRD4, at enhancers. One limitation of this study is that BRD4 mRNA undergoes alternative processing leading to long and short forms of the BRD4 protein. Importantly, the long form includes the C-terminal P-TEFb interaction domain that is required for the global release of Pol II under normal cellular conditions. In order to ensure the production of the essential long form of BRD4, we used CRISPR to target the C terminus of the long form of BRD4, which allows for continued production of the short form of BRD4, which more closely resembles BRD2 and BRD3. It is possible that, if the short form of BRD4 could be similarly targeted without disrupting the production of the long form, additional enhancer roles for BRD4 similar to BRD2's activity could be uncovered. Since clinical trials with BET inhibitors are ongoing for multiple cancer types, understanding the consequences of BET inhibition on the entire family in different cancer types expressing different levels of the various BET proteins is an important area for future investigation, as these findings could be important for stratifying BET inhibition to particular cancers relying on different BET proteins for their oncogenic programs.

Materials and methods

Antibodies

BRD2 (5848), BRD4 (13440), RPB1 (14958), HSP70 (4872), Actin (3700), and CDK9 (2316) were obtained from Cell Signaling Technology. BRD3 (#A302-368A) and AFF1 (#A302-345A) antibodies were obtained from Bethyl Laboratories. AFF4 (#14662-1-AP) antibody was obtained from Proteintech. Tubulin (#E7) was obtained from Developmental Studies Hybridoma Bank. HSP90 (#sc-7947) was obtained from Santa Cruz Biotechnology. H3 was generated in-house. Pol II Ser-2P (#04-1571) was obtained from Millipore Sigma. The rabbit anti-mAID antibody was generated at the Pocono Rabbit Farms and Laboratory. Rabbits were immunized with four synthetic peptides spanning the mAID sequence CPKDPAKPPAKAQVVGWP, PVRSYRKNVMVSC, CQKSSGGPEAAAFVKVS, and SMDGAPYLRKIDLRMYKC and conjugated to KLH using the cysteine. Three of the peptides that were immunogenic were used for affinity purification on SulfoLink resin (Thermo Fisher).

Cell culture

DLD-1 cells expressing OsTIR1 (Holland et al. 2012) were a gift from Dr. Dan Foltz. Cells were grown in DMEM media supplemented with 10% fetal bovine serum, 1% PenStrep, and 1% glutmax, as well as puromycin selection for the OsTIR1 transgene. Cells in normal condition were cultured in a 37°C incubator with 5% CO_2. For heat shock experiments, cells were treated with H_2O or 500 µM auxin for 2 h at 37°C before instantaneous heat shock (Mahat and Lis 2017) using conditioned prewarmed 42°C media and placed in a 42°C incubator for 1 h. HCT116 cells expressing OsTIR1were a gift from Dr. Masato T. Kanemaki (Natsume et al. 2016).

AID cell line generation

DLD-1 or HCT116 cells were transfected with a Cas9-expressing plasmid, PX330 (Addgene 42230) (Cong et al. 2013), carrying a guide RNA targeting 50 bp directly upstream of or downstream from the stop codon, and two donor plasmids. The donor plasmids were constructed using pBlueScript SK (II) as a backbone, and a left and right homology arm, ~300–500 bp each, flanking the mAID tag, and a selective antibiotic resistance gene cassette, either neomycin or hygromycin B. pMK286 (Addgene 72824) and pMK287 (Addgene 72825) were used to derive the mAID tag and antibiotic resistance gene cassette (Natsume et al. 2016). After 2 wk of drug selection using geneticin and hygromycin B, single-cell colonies were picked and validated by PCR and Western blot to select homozygous clones.

Western blotting

For whole-cell lysates, cells were washed with PBS once before lysing with 2× sample buffer added directly to plates. Nuclear extracts were made with the nuclear extract kit (Active Motif 40010) and then mixed with an equal volume of 4× sample buffer. Quantification of Western blotting was carried out with the ImageLab from Bio-Rad.

ChIP-seq

Cells were cross-linked with 1% PFA in PBS for 10 min at room temperature and were collected by scraping. Fixed mouse embryonic fibroblast cells were added as a spike-in at a 1:5 ratio. Sonication of the chromatin was performed using the Covaris E220 sonicator for 4 min, with 10% duty factor, 200 cycles per burst, and 140 peak intensity power. Immunoprecipitation was completed using 5 µL of Pol II antibody or 10 µL of the other antibodies, and immune complexes were collected with A/G-agarose beads (Santa Cruz Biotechnology) or Dynabeads Protein G (Invitrogen). DNA libraries were prepared using a KAPA HTP library prep kit and sequenced on the Illumina NextSeq 500 or NovaSeq 6000.

mRNA-seq

Cells were treated with or without auxin for 2 h in a 37°C incubator and were directly placed into a 42°C incubator for heat shock. Total RNAs were isolated using the RNeasy mini kit from Qiagen. mRNAs were isolated using a NEBNext poly(A) mRNA magnetic isolation module. RNA libraries were prepared using NEBNext Ultra II Directional RNA library preparation kit and sequenced on the Illumina NovaSeq 6000. Reads were aligned to the human genome (hg19) using Bowtie version 2.2.6.0 and a TopHat run (v2.1.0) (Langmead et al. 2009; Trapnell et al. 2009).

ChIP-seq analysis

Reads were aligned to the human genome (hg19) using Bowtie version 1.1.2. Peaks of mAID ChIP-seq were called using MACS2/2.1.0 with a threshold of q value = 0.01 (Zhang et al. 2008) and annotated with HOMER 4.10 (Heinz et al. 2010). Intervene 0.6.4 was used to generate the Venn diagrams (Khan and Mathelier 2017). Custom R scripts were used to select genes for further analysis that are transcribed by Pol II, have a minimum length of 2 kb, and are within at least 1 kb from other genes. Transcript coverage by Pol II for the promoter-proximal (100 bases upstream of and 300 bases downstream from the TSS), gene body, and full gene regions was calculated using bedtools/2.29.1 (Quinlan and Hall 2010). To find genes with the highest heat shock response, the full gene regions in wild-type cells were ordered by the $\log_2$ FC coverage ratio between 42°C and 37°C using deepTools 3.1.1 (Ramírez et al. 2016). k-means clustering (k = 4) was applied,

and the top induced cluster (227 genes) was selected for further analysis under different treatment protocols. The pause release ratio (PRR) was defined as the Pol II coverage in the gene body over the promoter-proximal region, modified from the traveling ratio (RT) (Reppas et al. 2006). Log_2PRR ECDF plots were generated using custom R scripts. Log_2RPKM in box plots were generated by counting the mapped reads at designated regions by featureCounts 2.0.1 (Liao et al. 2014). To compare affected genes in AFF1 and AFF4 double degron cells and KL-1 treated cells, genes from the two most heat shock-induced clusters (C1 and C2 in Supplemental Fig. S3A) were used for subtracting the 42°C versus 37°C log_2FC coverages of treated (KL-1 and auxin depletion of AFF1 and AFF4) and respective control samples and *k*-means clustered ($k = 3$) into "affected" and "nonaffected" groups for each treatment. Genes from each "affected" group were cross-referenced with the 227 HS-induced genes, resulting in 195 genes that are heat shock-induced and responsive to treatment with KL-1, while 181 heat shock-induced genes were responsive to the AFF1/4-AID treatment.

Data availability

ChIP-seq data has been deposited at GEO under accession number GSE145525 and will be available upon publication.

Acknowledgments

We thank the members of the Shilatifard laboratory and Dr. Marc Mendillo for helpful discussions. Y.A. was supported by the Japan Society for the Promotion of Science Research Fellowship for Young Scientists and the Uehara Memorial Foundation Research Fellowship. E.R.S. was supported by National Institutes of Health grant R50CA211428. Studies in the Shilatifard laboratory related to transcription elongation are funded by National Institutes of Health grant R01CA214035.

Author contributions: B.Z., Y.A., and A.P.S. performed experiments. M.I. and S.D. performed data analysis. E.J.R., D.Z., and N.K. performed the NGS studies. E.R.S. and A.S. designed experiments, discussed the results, analyzed data, and helped B.Z. write the manuscript.

References

Adelman K, Lis JT. 2012. Promoter-proximal pausing of RNA polymerase II: emerging roles in metazoans. *Nat Rev Genet* **13:** 720–731. doi:10.1038/nrg3293

Andersson R, Sandelin A. 2020. Determinants of enhancer and promoter activities of regulatory elements. *Nat Rev Genet* **21:** 71–87. doi:10.1038/s41576-019-0173-8

Bisgrove DA, Mahmoudi T, Henklein P, Verdin E. 2007. Conserved P-TEFb-interacting domain of BRD4 inhibits HIV transcription. *Proc Natl Acad Sci* **104:** 13690–13695. doi:10.1073/pnas.0705053104

Bitoun E, Davies KE. 2005. The robotic mouse: unravelling the function of AF4 in the cerebellum. *Cerebellum* **4:** 250–260. doi:10.1080/14734220500325897

Chen FX, Smith ER, Shilatifard A. 2018. Born to run: control of transcription elongation by RNA polymerase II. *Nat Rev Mol Cell Biol* **19:** 464–478. doi:10.1038/s41580-018-0010-5

Cong L, Ran FA, Cox D, Lin SL, Barretto R, Habib N, Hsu PD, Wu XB, Jiang WY, Marraffini LA, et al. 2013. Multiplex genome engineering using CRISPR/Cas systems. *Science* **339:** 819–823. doi:10.1126/science.1231143

Dawson MA, Prinjha RK, Dittmann A, Giotopoulos G, Bantscheff M, Chan WI, Robson SC, Chung CW, Hopf C, Savitski MM, et al. 2011. Inhibition of BET recruitment to chromatin as an effective treatment for MLL-fusion leukaemia. *Nature* **478:** 529–533. doi:10.1038/nature10509

Filippakopoulos P, Qi J, Picaud S, Shen Y, Smith WB, Fedorov O, Morse EM, Keates T, Hickman TT, Felletar I, et al. 2010. Selective inhibition of BET bromodomains. *Nature* **468:** 1067–1073. doi:10.1038/nature09504

He N, Liu M, Hsu J, Xue Y, Chou S, Burlingame A, Krogan NJ, Alber T, Zhou Q. 2010. HIV-1 Tat and host AFF4 recruit two transcription elongation factors into a bifunctional complex for coordinated activation of HIV-1 transcription. *Mol Cell* **38:** 428–438. doi:10.1016/j.molcel.2010.04.013

He N, Chan CK, Sobhian B, Chou S, Xue Y, Liu M, Alber T, Benkirane M, Zhou Q. 2011. Human polymerase-associated factor complex (PAFc) connects the super elongation complex (SEC) to RNA polymerase II on chromatin. *Proc Natl Acad Sci* **108:** E636–E645. doi:10.1073/pnas.1107107108

Heinz S, Benner C, Spann N, Bertolino E, Lin YC, Laslo P, Cheng JX, Murre C, Singh H, Glass CK. 2010. Simple combinations of lineage-determining transcription factors prime *cis*-regulatory elements required for macrophage and B cell identities. *Mol Cell* **38:** 576–589. doi:10.1016/j.molcel.2010.05.004

Holland AJ, Fachinetti D, Han JS, Cleveland DW. 2012. Inducible, reversible system for the rapid and complete degradation of proteins in mammalian cells. *Proc Natl Acad Sci* **109:** E3350–E3357. doi:10.1073/pnas.1216880109

Hsu SC, Blobel GA. 2017. The role of bromodomain and extraterminal motif (BET) proteins in chromatin structure. *Cold Spring Harb Symp Quant Biol* **82:** 37–43. doi:10.1101/sqb.2017.82.033829

Hsu SC, Gilgenast TG, Bartman CR, Edwards CR, Stonestrom AJ, Huang P, Emerson DJ, Evans P, Werner MT, Keller CA, et al. 2017. The BET protein BRD2 cooperates with CTCF to enforce transcriptional and architectural boundaries. *Mol Cell* **66:** 102–116.e7. doi:10.1016/j.molcel.2017.02.027

Hussong M, Kaehler C, Kerick M, Grimm C, Franz A, Timmermann B, Welzel F, Isensee J, Hucho T, Krobitsch S, et al. 2017. The bromodomain protein BRD4 regulates splicing during heat shock. *Nucleic Acids Res* **45:** 382–394. doi:10.1093/nar/gkw729

Izumi K, Nakato R, Zhang Z, Edmondson AC, Noon S, Dulik MC, Rajagopalan R, Venditti CP, Gripp K, Samanich J, et al. 2015. Germline gain-of-function mutations in AFF4 cause a developmental syndrome functionally linking the super elongation complex and cohesin. *Nat Genet* **47:** 338–344. doi:10.1038/ng.3229

Jang MK, Mochizuki K, Zhou MS, Jeong HS, Brady JN, Ozato K. 2005. The bromodomain protein Brd4 is a positive regulatory component of P-TEFb and stimulates RNA polymerase II-dependent transcription. *Mol Cell* **19:** 523–534. doi:10.1016/j.molcel.2005.06.027

Kanno T, Kanno Y, LeRoy G, Campos E, Sun HW, Brooks SR, Vahedi G, Heightman TD, Garcia BA, Reinberg D, et al. 2014. BRD4 assists elongation of both coding and enhancer RNAs by interacting with acetylated histones. *Nat Struct Mol Biol* **21:** 1047–1057. doi:10.1038/nsmb.2912

Khan A, Mathelier A. 2017. Intervene: a tool for intersection and visualization of multiple gene or genomic region sets. *BMC Bioinformatics* **18:** 287. doi:10.1186/s12859-017-1708-7

Langmead B, Trapnell C, Pop M, Salzberg SL. 2009. Ultrafast and memory-efficient alignment of short DNA sequences to the human genome. *Genome Biol* **10:** R25. doi:10.1186/gb-2009-10-3-r25

Li WB, Notani D, Rosenfeld MG. 2016. Enhancers as non-coding RNA transcription units: recent insights and future perspectives. *Nat Rev Genet* **17:** 207–223. doi:10.1038/nrg.2016.4

Li S, Prasanna X, Salo VT, Vattulainen I, Ikonen E. 2019. An efficient auxin-inducible degron system with low basal degradation in human cells. *Nat Methods* **16:** 866–869. doi:10.1038/s41592-019-0512-x

Liang K, Smith ER, Aoi Y, Stoltz KL, Katagi H, Woodfin AR, Rendleman EJ, Marshall SA, Murray DC, Wang L, et al. 2018. Targeting processive transcription elongation via SEC disruption for MYC-induced cancer therapy. *Cell* **175:** 766–779.e17. doi:10.1016/j.cell.2018.09.027

Liao Y, Smyth GK, Shi W. 2014. featureCounts: an efficient general purpose program for assigning sequence reads to genomic features. *Bioinformatics* **30:** 923–930. doi:10.1093/bioinformatics/btt656

Lin C, Smith ER, Takahashi H, Lai KC, Martin-Brown S, Florens L, Washburn MP, Conaway JW, Conaway RC, Shilatifard A. 2010. AFF4, a component of the ELL/P-TEFb elongation complex and a shared subunit of MLL chimeras, can link transcription elongation to leukemia. *Mol Cell* **37:** 429–437. doi:10.1016/j.molcel.2010.01.026

Lin C, Garrett AS, De Kumar B, Smith ER, Gogol M, Seidel C, Krumlauf R, Shilatifard A. 2011. Dynamic transcriptional events in embryonic stem cells mediated by the super elongation complex (SEC). *Genes Dev* **25:** 1486–1498. doi:10.1101/gad.2059211

Lis JT, Mason P, Peng J, Price DH, Werner J. 2000. P-TEFb kinase recruitment and function at heat shock loci. *Genes Dev* **14:** 792–803.

Lovén J, Hoke HA, Lin CY, Lau A, Orlando DA, Vakoc CR, Bradner JE, Lee TI, Young RA. 2013. Selective inhibition of tumor oncogenes by disruption of super-enhancers. *Cell* **153:** 320–334. doi:10.1016/j.cell.2013.03.036

Lu H, Li Z, Zhang W, Schulze-Gahmen U, Xue Y, Zhou Q. 2015a. Gene target specificity of the super elongation complex (SEC) family: how HIV-1 Tat employs selected SEC members to activate viral transcription. *Nucleic Acids Res* **43:** 5868–5879. doi:10.1093/nar/gkv541

Lu J, Qian Y, Altieri M, Dong H, Wang J, Raina K, Hines J, Winkler JD, Crew AP, Coleman K, et al. 2015b. Hijacking the E3 ubiquitin ligase cereblon to efficiently target BRD4. *Chem Biol* **22:** 755–763. doi:10.1016/j.chembiol.2015.05.009

Luo Z, Lin C, Guest E, Garrett AS, Mohaghegh N, Swanson S, Marshall S, Florens L, Washburn MP, Shilatifard A. 2012a. The super elongation complex family of RNA polymerase II elongation factors: gene target specificity and transcriptional output. *Mol Cell Biol* **32:** 2608–2617. doi:10.1128/MCB.00182-12

Luo Z, Lin C, Shilatifard A. 2012b. The super elongation complex (SEC) family in transcriptional control. *Nat Rev Mol Cell Biol* **13:** 543–547. doi:10.1038/nrm3417

Mahat DB, Lis JT. 2017. Use of conditioned media is critical for studies of regulation in response to rapid heat shock. *Cell Stress Chaperones* **22:** 155–162. doi:10.1007/s12192-016-0737-x

Mahat DB, Salamanca HH, Duarte FM, Danko CG, Lis JT. 2016. Mammalian heat shock response and mechanisms underlying its genome-wide transcriptional regulation. *Mol Cell* **62:** 63–78. doi:10.1016/j.molcel.2016.02.025

Muhar M, Ebert A, Neumann T, Umkehrer C, Jude J, Wieshofer C, Rescheneder P, Lipp JJ, Herzog VA, Reichholf B, et al. 2018. SLAM-seq defines direct gene-regulatory functions of the BRD4-MYC axis. *Science* **360:** 800–805. doi:10.1126/science.aao2793

Natsume T, Kiyomitsu T, Saga Y, Kanemaki MT. 2016. Rapid protein depletion in human cells by auxin-inducible degron tagging with short homology donors. *Cell Rep* **15:** 210–218. doi:10.1016/j.celrep.2016.03.001

Nguyen VT, Kiss T, Michels AA, Bensaude O. 2001. 7SK small nuclear RNA binds to and inhibits the activity of CDK9/cyclin T complexes. *Nature* **414:** 322–325. doi:10.1038/35104581

Ni Z, Saunders A, Fuda NJ, Yao J, Suarez JR, Webb WW, Lis JT. 2008. P-TEFb is critical for the maturation of RNA polymerase II into productive elongation in vivo. *Mol Cell Biol* **28:** 1161–1170. doi:10.1128/MCB.01859-07

Nishimura K, Fukagawa T, Takisawa H, Kakimoto T, Kanemaki M. 2009. An auxin-based degron system for the rapid depletion of proteins in nonplant cells. *Nat Methods* **6:** 917–922. doi:10.1038/nmeth.1401

Peterlin BM, Price DH. 2006. Controlling the elongation phase of transcription with P-TEFb. *Mol Cell* **23:** 297–305. doi:10.1016/j.molcel.2006.06.014

Price DH. 2000. P-TEFb, a cyclin-dependent kinase controlling elongation by RNA polymerase II. *Mol Cell Biol* **20:** 2629–2634. doi:10.1128/MCB.20.8.2629-2634.2000

Quinlan AR, Hall IM. 2010. BEDTools: a flexible suite of utilities for comparing genomic features. *Bioinformatics* **26:** 841–842. doi:10.1093/bioinformatics/btq033

Ramírez F, Ryan DP, Grüning B, Bhardwaj V, Kilpert F, Richter AS, Heyne S, Dündar F, Manke T. 2016. deepTools2: a next generation web server for deep-sequencing data analysis. *Nucleic Acids Res* **44:** W160–W165. doi:10.1093/nar/gkw257

Reppas NB, Wade JT, Church GM, Struhl K. 2006. The transition between transcriptional initiation and elongation in *E. coli* is highly variable and often rate limiting. *Mol Cell* **24:** 747–757. doi:10.1016/j.molcel.2006.10.030

Sathyan KM, McKenna BD, Anderson WD, Duarte FM, Core L, Guertin MJ. 2019. An improved auxin-inducible degron system preserves native protein levels and enables rapid and specific protein depletion. *Genes Dev* **33:** 1441–1455. doi:10.1101/gad.328237.119

Schoenfelder S, Fraser P. 2019. Long-range enhancer-promoter contacts in gene expression control. *Nat Rev Genet* **20:** 437–455. doi:10.1038/s41576-019-0128-0

Schulze-Gahmen U, Upton H, Birnberg A, Bao K, Chou S, Krogan NJ, Zhou Q, Alber T. 2013. The AFF4 scaffold binds human P-TEFb adjacent to HIV Tat. *Elife* **2:** e00327. doi:10.7554/eLife.00327

Shilatifard A, Lane WS, Jackson KW, Conaway RC, Conaway JW. 1996. An RNA polymerase II elongation factor encoded by the human ELL gene. *Science* **271:** 1873–1876. doi:10.1126/science.271.5257.1873

Shilatifard A, Duan DR, Haque D, Florence C, Schubach WH, Conaway JW, Conaway RC. 1997. ELL2, a new member of an ELL family of RNA polymerase II elongation factors. *Proc Natl Acad Sci* **94:** 3639–3643. doi:10.1073/pnas.94.8.3639

Smith ER, Winter B, Eissenberg JC, Shilatifard A. 2008. Regulation of the transcriptional activity of poised RNA polymerase II by the elongation factor ELL. *Proc Natl Acad Sci* **105:** 8575–8579. doi:10.1073/pnas.0804379105

Smith E, Lin C, Shilatifard A. 2011. The super elongation complex (SEC) and MLL in development and disease. *Genes Dev* **25:** 661–672. doi:10.1101/gad.2015411

Sobhian B, Laguette N, Yatim A, Nakamura M, Levy Y, Kiernan R, Benkirane M. 2010. HIV-1 Tat assembles a multifunctional transcription elongation complex and stably associates with the 7SK snRNP. *Mol Cell* **38:** 439–451. doi:10.1016/j.molcel.2010.04.012

Takahashi H, Parmely TJ, Sato S, Tomomori-Sato C, Banks CAS, Kong SE, Szutorisz H, Swanson SK, Martin-Brown S, Washburn MP, et al. 2011. Human mediator subunit MED26 functions as a docking site for transcription elongation factors. *Cell* **146:** 92–104. doi:10.1016/j.cell.2011.06.005

Trapnell C, Pachter L, Salzberg SL. 2009. TopHat: discovering splice junctions with RNA-seq. *Bioinformatics* **25:** 1105–1111. doi:10.1093/bioinformatics/btp120

Winter GE, Buckley DL, Paulk J, Roberts JM, Souza A, Dhe-Paganon S, Bradner JE. 2015. Phthalimide conjugation as a strategy for in vivo target protein degradation. *Science* **348:** 1376–1381. doi:10.1126/science.aab1433

Winter GE, Mayer A, Buckley DL, Erb MA, Roderick JE, Vittori S, Reyes JM, di Iulio J, Souza A, Ott CJ, et al. 2017. BET bromodomain proteins function as master transcription elongation factors independent of CDK9 recruitment. *Mol Cell* **67:** 5–18.e19. doi:10.1016/j.molcel.2017.06.004

Yik JH, Chen R, Nishimura R, Jennings JL, Link AJ, Zhou Q. 2003. Inhibition of P-TEFb (CDK9/Cyclin T) kinase and RNA polymerase II transcription by the coordinated actions of HEXIM1 and 7SK snRNA. *Mol Cell* **12:** 971–982. doi:10.1016/S1097-2765(03)00388-5

Zhang Y, Liu T, Meyer CA, Eeckhoute J, Johnson DS, Bernstein BE, Nussbaum C, Myers RM, Brown M, Li W, et al. 2008. Model-based analysis of ChIP-seq (MACS). *Genome Biol* **9:** R137. doi:10.1186/gb-2008-9-9-r137

Zhou Q, Yik JH. 2006. The Yin and Yang of P-TEFb regulation: implications for human immunodeficiency virus gene expression and global control of cell growth and differentiation. *Microbiol Mol Biol Rev* **70:** 646–659. doi:10.1128/MMBR.00011-06

Zuber J, Shi J, Wang E, Rappaport AR, Herrmann H, Sison EA, Magoon D, Qi J, Blatt K, Wunderlich M, et al. 2011. RNAi screen identifies Brd4 as a therapeutic target in acute myeloid leukaemia. *Nature* **478:** 524–528. doi:10.1038/nature10334